Long-Range Effects of Noble Metals on the Photocatalytic Properties of Titanium Dioxide

ARTICLE *in* THE JOURNAL OF PHYSICAL CHEMISTRY B · FEBRUARY 2003

Impact Factor: 3.3 · DOI: 10.1021/jp026940i

2 AUTHORS:

Hossam Haick
Technion - Israel Institute of Technology
158 PUBLICATIONS **4,422** CITATIONS
SEE PROFILE

Yaron Paz
Technion - Israel Institute of Technology
58 PUBLICATIONS **1,603** CITATIONS
SEE PROFILE

Long-Range Effects of Noble Metals on the Photocatalytic Properties of Titanium Dioxide

Hossam Haick and Yaron Paz*

Department of Chemical Engineering and the Institute of Catalysis, Technion-Israel Institute of Technology, Haifa 32000, Israel

Received: September 8, 2002; In Final Form: December 29, 2002

Well-defined structures comprised of alternating microstripes of noble metals (Au, Pt) and TiO_2, covered with self-assembled monolayers (SAMs), are used to study long-range metallic effects on the photodegradation of the monolayers. It was found that under certain conditions, the presence of a metal in the vicinity of the photocatalyst does not increase its photoefficiency but, in fact, might reduce it significantly, in comparison with a bare photocatalyst. This effect depends on the size of the domains, as well as on humidity and the type of metal. It is suggested that although metal-induced charge separation is beneficial in promoting the production of hydroxyl radicals needed for the first steps of the degradation process, charge separation might also become detrimental under conditions that decrease the back-diffusion of reduced species, such as hydroperoxy radicals, needed at later stages of the degradation process.

1. Introduction

Heterogeneous photocatalysis, using titanium dioxide as the photocatalyst of choice, is a useful technique for the degradation of many contaminants in air, in water, or on solid surfaces.[1] The general scheme for the photocatalytic destruction of organic compounds involves the excitation of this semiconductor by irradiation with supraband gap photons and migration of the electron−hole pairs to the surface of the photocatalyst, where the holes may react with adsorbed H_2O or OH^- to form hydroxyl radicals. Similarly, the electrons may be trapped in oxygen vacancies deep traps[2] or in shallow traps on surface-hydroxylated sites. For most organic materials, destruction occurs through an oxidation mechanism where the hydroxyl radicals attack the organic compound to give, for example, alkyl radicals, which undergo secondary reactions, for example, with superoxide radicals,[3] to form stable molecules.[4] Direct oxidation by holes was also observed, especially for compounds with no hydrogen atoms available for abstraction by OH radicals, such as dichloroacetate,[5] or when the concentration of the contaminants is very high and molecules are strongly adsorbed on the surface.[6,7]

Numerous investigations have reported that the addition of noble metals such as gold,[8,9] platinum,[10,11] silver,[12] or palladium[13] may enhance the overall photoefficiency of TiO_2. This effect is almost conclusively attributed to a reduction in the recombination rate due to better charge separation between the electrons, which accumulate on the metal, and the holes, which remain on the photocatalyst surface.[14] Several groups have proposed that the charge separation is the outcome of a Schottky barrier at the TiO_2−metal interface.[9,15] However, for nanoparticles, it is quite difficult to assume band-bending effects taken that the width of the space charge layer is in the range of 200−700 Å.[16]

The effect of platinum and gold on photocatalysis is often mixed with thermal catalytic effects, although the two mechanisms can be separated by their different dependence on the temperature. A classical example is CO oxidation, where the increased rate found at elevated temperatures was attributed solely to thermal effects, related to oxygen adsorption and spillover.[17] In fact, thermal and photocatalytic (electronic) mechanisms may operate synergistically as was found in the case of acetaldehyde, where Pt prevents the deactivation of titanium dioxide during photocatalysis by supplying spilt-over oxygen.[18]

The beneficial effect of noble metals depends to a large extent on the loading. For example, the photoinduced H_2 production from ethylene glycol peaked at a loading of 2.3 wt % Au.[19] Likewise, the rate of photooxidation of 2-propanol and (*S*)-lysine, which was negligible without Pt, increased drastically with Pt loading up to ca. 0.3 wt % and then slightly decreased.[20] The fact that the optimal amounts of metals were obtained at relatively low loadings, i.e., at relatively low surface coverage, suggests that this optimum is not simply due to a decrease in the available surface area but, instead, may reflect some recombinative activity of the metallic islands,[21] possibly through a layer of metallic ions, existing at the TiO_2−metal interface.[22]

Among the factors that play a dominant role in determining the activity of metal−TiO_2 hybrid structures is the deposition method.[23] That way, it was reported that the efficiency of Au/TiO_2 structures in H_2 photoproduction decreased in the order photodeposition, deposition−precipitation, impregnation, and simple mixing. The activity of Pt/TiO_2 samples was less sensitive to the preparation method and decreased in the order Pt/TiO_2 (photodeposition) > Pt/TiO_2 (deposition−precipitation) ≈ Pt/TiO_2 (impregnation).[24]

The dependence of the enhancement on the loading and on the deposition technique suggests that the mechanism of nucleation and growth of the metallic islands may play a dominant role. Indeed, absence of platinum enhancement in the photooxidation of CO to CO_2 at low temperatures (where thermal catalysis effects are negligible) was explained in terms of Pt cluster nucleation on defect sites, thus reducing the number of chemisorbed O_2 molecules available for the photooxidation reaction.[25]

All of the above-mentioned works were performed with nanosized metallic islands, characterized by very short diffusion lengths for chemical species and for charge carriers and by a

* To whom correspondence should be addressed. Tel: +972-4-8292486. Fax: +972-4-8230476. E-mail: paz@tx.technion.ac.il.

10.1021/jp026940i CCC: $25.00
Published on Web 02/12/2003

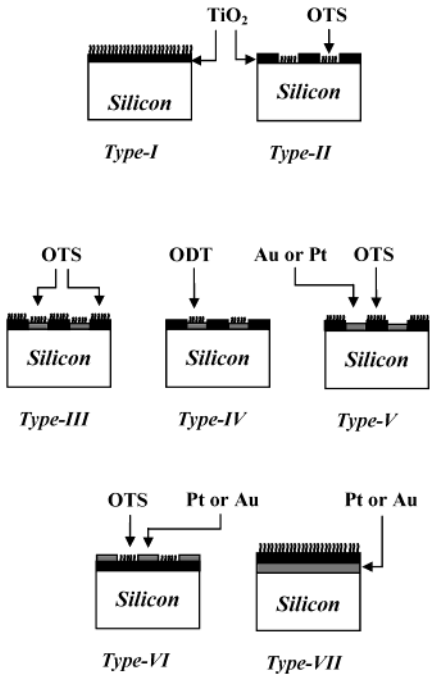

Figure 1. The different types of hybrid structures.

very high interface to area ratio. While actual photocatalysts may use such structures in real life, we believe that decoupling between interfacial and bulk effects may provide basic understanding that might be utilized at a later stage. Such a level of understanding requires us to fix the location of the contaminants at a known, predetermined distance from the metal islands during the photocatalytic experiments.

In this paper, well-defined structures comprised of alternating microstripes of TiO_2 and metal (gold, platinum, or aluminum), covered with self-assembled monolayers (SAMs), are used to study long-range metallic effects on the photodegradation of the monolayers. It was found that under certain conditions, not only the presence of a metal in the vicinity of the photocatalyst does not increase its photoefficiency but, in fact, might reduce it significantly, in comparison with a bare photocatalyst.

2. Experimental Section

2.a. Sample Preparation and Characterization. Seven types of samples were prepared (Figure 1). Type I and type VII were nonpatterned samples, whereas type II, type III, type IV, type V, and type VI consisted of microstripes structures. In each of these types, several stripe widths were used, usually in the range of 5−160 μm. All of the stripes in a certain wafer had the same width, to enable averaging over a large number of stripes. Unless otherwise specified, the exposed area of titanium dioxide in each of the patterned wafers was kept constant at 50%, regardless of the stripes' width.

Type I Samples. Type I samples were nonpatterned TiO_2-coated silicon wafers, covered with monolayers of octadecyltrichlorosilane (OTS). The preparation of the type I samples included the coating of a set of 1 inch silicon wafers (P-type (111), polished on both sides, 3000 Ω cm, Topsil, U.S.A.) by a thin (70 nm), well-adhered, nanocrystalline TiO_2 (anatase) film, produced by a sol−gel process, similar to the one used by us for the preparation of self-cleaning glass[26,27] but with a calcination temperature of 450 °C. Cross-linked SAMs of OTS ($CH_3(CH_2)_{17}SiCl_3$) were then chemisorbed by the self-assembly method.[28] These monolayers are known to consist of long alkyl chains attached covalently to the surface of oxides by siloxane bonds (Si−O−Si for a silicon oxide substrate, Si−O−Ti for a titanium dioxide substrate), where adjacent chains are cross-linked by Si−O−Si bonds.

Type II Samples. Type II samples consisted of OTS monolayers, chemisorbed only on silicon domains in structures made of alternating, repetitive microstripes of silicon and titanium dioxide. The first step in the preparation of these samples was the formation of Si/TiO_2 hybrid structures as described before.[29,30] The preparation procedure included patterning of a TiO_2 layer on silicon (Figure 2), to obtain alternating stripes of titania and silicon, followed by OTS chemisorption over the whole wafer, and O_2−plasma ashing of the monolayer from the titanium dioxide domains, while protecting the monolayer on the silicon domains. To ensure that the surface obtained after the stripping of the protecting photoresistant layer consisted of OTS attached only to the selected silicon domains and to ascertain that the OTS layer on the silicon domains was not damaged during the last steps, microprobe Fourier transform infrared (FTIR) measurements of single stripes (both Si and TiO_2) were taken prior to photoresistant coating and after photoresistant stripping.

Type III Samples. Type III samples consisted of OTS monolayers, chemisorbed on substrates made of alternating, repetitive microstripes of aluminum and titanium dioxide. Following the formation of Si/TiO_2 hybrid structures, a thin film of aluminum (750 Å in thickness) was deposited by evaporation and patterned onto the silicon microstripes by a conventional lift-off process. Chemisorption of monolayers of OTS on the titanium dioxide and on the (native oxide of) aluminum completed the preparation scheme of this type.

Type IV Samples. Type IV samples consisted of alternating, repetitive microstripes of gold (or platinum) and TiO_2. In these samples, the metal stripes, but not the TiO_2 stripes, were covered with monolayers of octadecanethiol (ODT, $CH_3(CH_2)_{17}SH$). The preparation of these samples was similar to that of type III samples except for replacing the aluminum with a thin (80 Å) underlayer of titanium onto which 750 Å thick gold (or platinum) films were deposited by evaporation. The titanium layer was used to enhance the adhesion of the metal layers to the silicon substrate. Monolayers of ODT were then chemisorbed from an alcoholic solution by the self-assembly technique. These molecules are known to bind to metallic substrates through their thiolate groups, thus creating close-packed, ordered, stable monolayers.[31]

Type V Samples. Type V samples consisted of alternating structures made of metallic microstripes (either gold or platinum) and titanium dioxide microstripes covered with a monolayer of OTS, known to be formed on oxides but not on metals. The preparation procedure was the same as that used for the preparation of type IV samples (see Figure 2), except for the type of monolayer used (OTS on TiO_2 instead of ODT on Au or Pt).

Type VI Samples. Similar to type V samples, type VI samples consisted of alternating stripes of metal and titanium dioxide, where the latter was covered with a monolayer of OTS. Unlike type V samples, where the metallic stripes were evaporated on the silicon substrate, the metallic stripes in the type VI samples were deposited on a titanium dioxide layer (see Figures 1 and 2). The preparation procedure was similar to the one described for type V, except for the lift-off step, which was carried out immediately after the photolithographic step.

Type VII Samples. Type VII samples were similar to type I samples (i.e., OTS on a TiO_2 layer in a nonpatterned surface), except for a metallic layer (Au or Pt, 1500 Å in thickness)

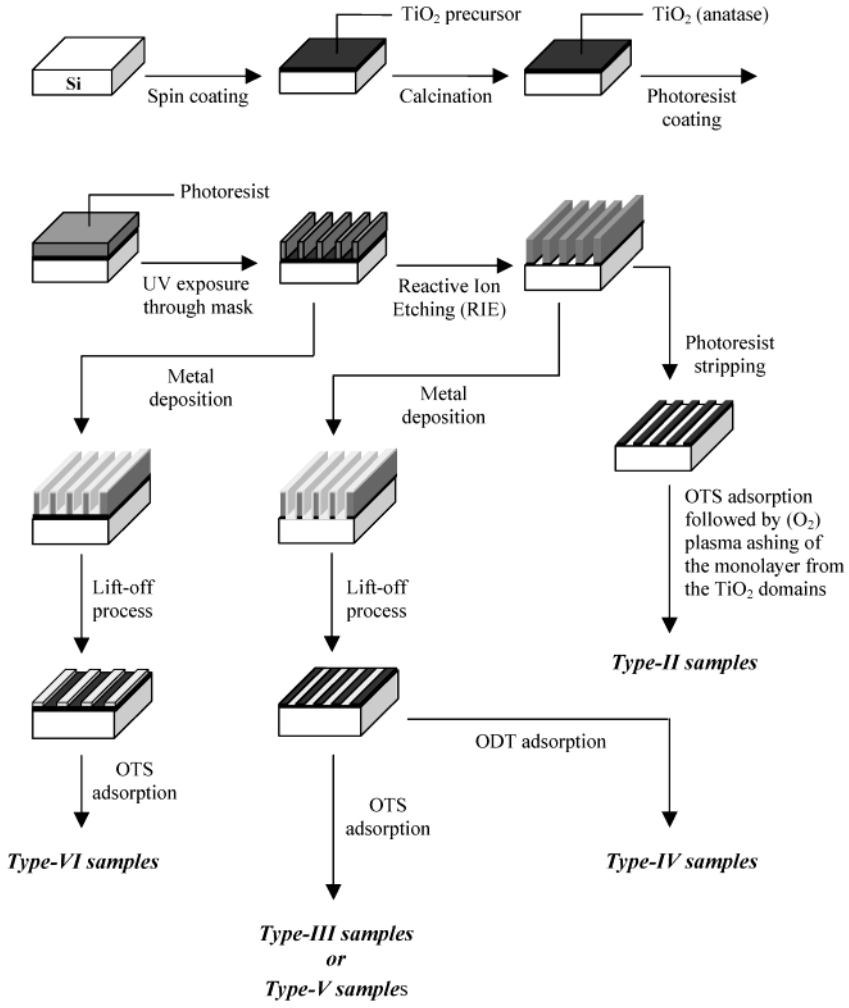

Figure 2. Samples' preparation scheme.

embedded underneath the titanium dioxide layer. The preparation of these samples included the evaporation of a thin (80 Å) titanium film on the silicon wafers prior to evaporation of the metal layer.

2.b. Photodegradation Measurements. The photodegradation experiments for all types of samples were held in situ, inside the sample compartment of an FTIR machine, under controlled temperature and environment (dry air and air with 40% relative humidity (RH)). The samples were illuminated by UV-254 nm light, using an UV pencil lamp (Spectroline, model 11SC-1, Spectronics Corporation, U.S.A.). Unless otherwise specified, the illumination power at the wafers' surface was 0.09 mW cm^{-2}. The photodegradation kinetics of the monolayers was determined by integrating the absorbance of the C−H stretch envelope (i.e., CH_2(a), CH_2(s), CH_3(a), CH_3(s)) in the FTIR spectra (Bruker IFS55, measured with 4 cm^{-1} resolution). Samples where the monolayers were chemisorbed on IR transparent medium (i.e., type I, type II, type V, and type VI) were measured by direct absorption mode, whereas samples on IR opaque substrates (i.e., type III, type IV, and type VII) were measured with a specular reflectance accessory at an incident angle of 45°. It is noteworthy that specular reflectance measurements of type I samples (OTS on nonpatterned TiO_2 on silicon) did not yield any signal at all, thus ensuring that the reflectance signal in the type III samples originated only from OTS molecules that were chemisorbed on the aluminum and not from OTS molecules that were chemisorbed on the TiO_2 domains. In addition, care was taken to ensure that the silicon backside of the wafers in all samples was free of any chemisorbed molecules prior to the beginning of measurements and that all types of samples were free of any contamination prior to the chemisorption of the monolayers.

3. Results

Figure 3 presents the C−H stretch envelope in the spectrum of a type I sample. Note the decrease in C−H stretch peaks upon exposure to the UV light. A total disappearance of the signal can be noticed following 49 minutes of exposure. In contrast, OTS films on silicon wafers without TiO_2 did not reveal any deterioration following exposure to the UV light under the same conditions, verifying that the presence of titanium dioxide was a prerequisite for this degradation process to happen.

Figure 4 shows the degradation kinetics of OTS monolayers located in the vicinity of titanium dioxide, as obtained by integrating the C−H stretch envelope of their spectra. Two traces are presented as follows: a type II sample (OTS on Si), made of stripes of 80 μm in width, and a type III sample (OTS on Al), made of stripes of 40 μm in width. For clarity, results are given in normalized units relative to the integrated intensity prior to exposure. Evidently, both monolayers were photodegraded as a result of illuminating the titanium dioxide stripes located in their vicinity. Because the monolayers are strongly bound to the surface by covalent bonds, this observation points out the fact that oxidizing species formed on the titanium dioxide domains can out-diffuse from the photocatalytic domains, where

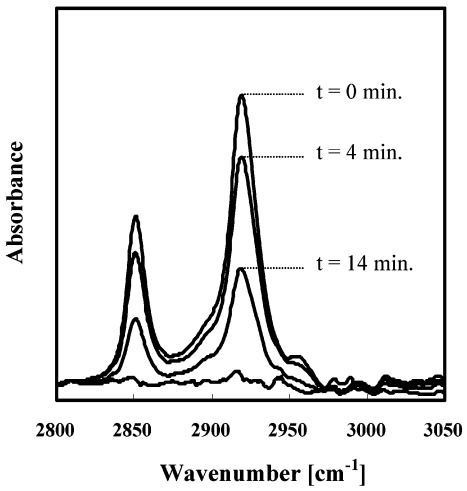

Figure 3. FTIR direct absorption spectra of OTS on type I samples, prior to exposure and following 4, 14, and 49 min of exposure to UV light.

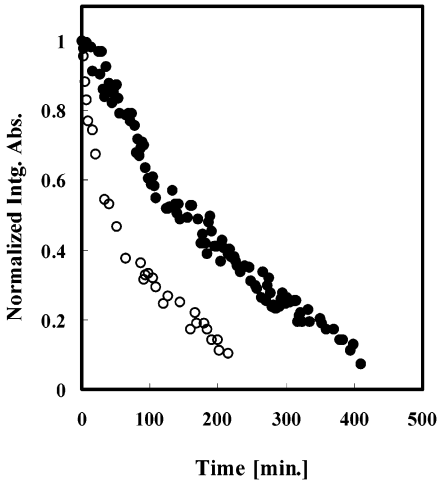

Figure 4. Normalized integrated absorption of the C−H stretch envelope of OTS as a function of UV exposure time for 80 μm stripes' width type II samples (○) and for 40 μm stripes' width type III samples (●).

they are formed, into adjacent inert domains (silicon or aluminum) where they participate in the oxidation of the OTS molecules.[29] The figure also demonstrates that the inert surface has a dominant role in the degradation kinetics: complete disappearance of the OTS signal on silicon was obtained after 200 minutes of exposure, whereas the time needed for complete disappearance of OTS on aluminum required no less than 400 minutes. This difference in the degradation rates is even more pronounced if one takes into consideration that the width of the silicon domains in the example shown in Figure 4 was larger than that of the aluminum domains, such that the averaged diffusion length of the oxidizing species on the silicon was larger than the averaged diffusion length on the aluminum surface.

That the type of inert surface located in the vicinity of the photocatalytic domains has a crucial role in determining the degradation rate of attached molecules is further demonstrated in Figure 5. Here, the integrated intensity of the C−H stretch envelope of ODT on gold and on platinum stripes located at the vicinity of titanium dioxide (type IV samples) is shown as a function of UV exposure time. The ODT monolayers are identical homologues to OTS (both are made of alkyl chains containing 17 methylenes and one methyl group); hence, one could have expected similar degradation rates. Instead, the

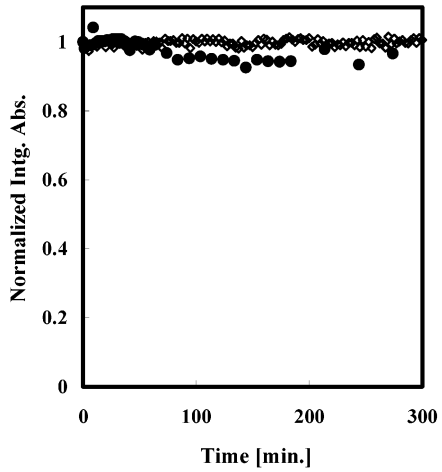

Figure 5. Normalized integrated absorption of ODT monolayer adsorbed on type IV samples as a function of UV exposure time. (●) Au/TiO_2 hybrid structures, stripes' width of 2.5 μm, 1 mW cm^{-2} UV flux, 27% RH. (◇) Pt/TiO_2 hybrid structures, stripes' width of 2.5 μm, 0.09 mW cm^{-2} UV flux, 8% RH.

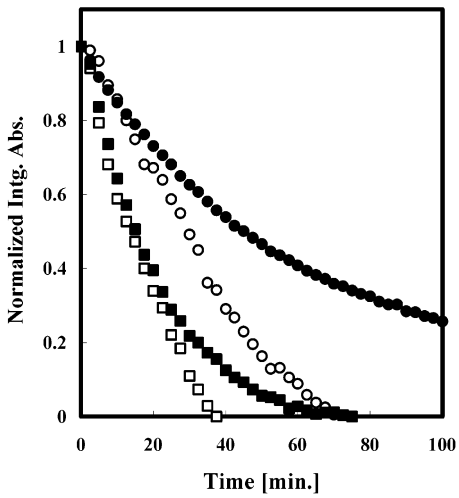

Figure 6. Normalized integrated absorption of OTS monolayer adsorbed on type I samples (○) and on type VII samples consisting of Si−Au−TiO_2 (●), Si−Pt−TiO_2 (□), and Si−TiO_2−Au−TiO_2 (■) layers.

photodegradation rate was found to be practically nil, for both platinum and gold substrates, even with very narrow domains (2.5 μm) or with UV flux that was 10 times larger than the UV flux used with type II and type III samples. The same results were obtained also with other stripes' widths or UV fluxes.

To decouple between pure electronic effects of noble metals, namely, charge separation, and spillover or any other chemical effects, the photodegradation of SAMs on titanium dioxide was studied in structures containing buried layers of either gold or platinum (Figure 6). Here, elemental analysis of the front TiO_2 surface, which did not reveal any Pt, verified that this metal did not diffuse all the way through the nascent TiO_2 film during calcination. It is noteworthy that although platinum may form silicides with silicon at the calcination temperature, no silicon was found by argon sputtering-assisted auger electron spectroscopy (AES) at the platinum/TiO_2 interface. The situation with gold was somehow more complex. Not only that the same structure did not yield any improvement in the degradation rate but, in fact, the presence of the buried layer was detrimental. A sputtering/AES study found that during calcination, silicon atoms diffuse through the gold and form a thick (approximately 0.5

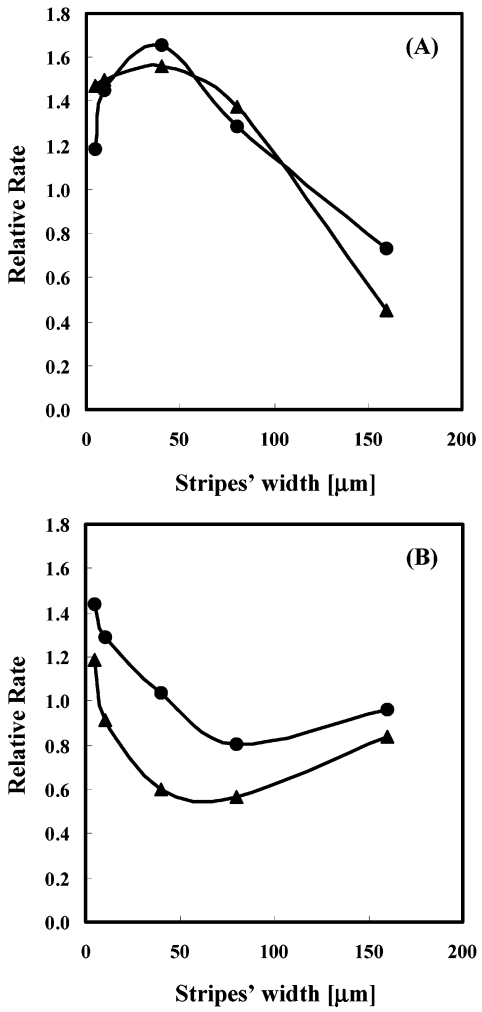

Figure 7. Degradation rates at 20% consumption, relative to those of type I samples, as a function of the stripes' width. All measurements (including those of type I) were taken under 40% RH. (A) Type V [Pt] (▲) and type VI [Pt] (●). (B) Type V [Au] (▲) and type VI [Au] (●).

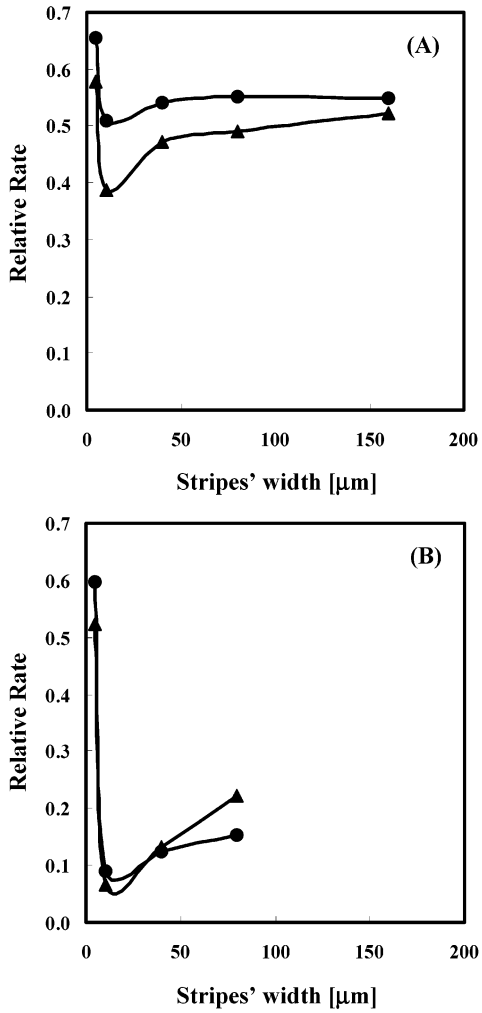

Figure 8. Degradation rates at 20% consumption, relative to those of type I samples, as a function of the stripes' width. All measurements (including those of type I) were taken under 1% RH. (A) Type V [Pt] (▲) and type VI [Pt] (●). (B) Type V [Au] (▲) and type VI [Au] (●).

μm) layer of silicon dioxide, which is enriched with ("nonproductive") titanium near the interface between the titanium dioxide and the newly formed silica. This was not a simple Fickean type of diffusion since the amount of silicon in the middle of the gold layer was lower than across that layer. Such a leaching-out of silicon atoms by gold to form silicon oxides is documented in the literature and was explained in terms of formation of nonstable Au−Si silicides.[32] Indeed, once an intermediate layer between the silicon and the gold was introduced, not only did the detrimental effect of the buried gold disappear but also an enhancement in the photocatalytic degradation of OTS due to the presence of gold was observed (Figure 6, filled squares).

Long-range effects of metals located at the air-exposed surface of the catalyst were studied by measuring the photodegradation of OTS chemisorbed on titanium dioxide microstripes (type V and type VI samples). To characterize each kinetics by representing values, the normalized integrated absorbance vs time curves were fitted into a tri-exponential fit ($R^2 > 0.97$), which was then differentiated analytically to give the photodegradation rate as a function of reaction coordinate. Figure 7 presents the rates, calculated at a point where 20% of the initial OTS was consumed, as a function of width of the stripes, for measurements done under RH of 40% and with stripes of platinum (Figure 7A) or gold (Figure 7B). For clarity, the rates are presented relative to the rate of type I samples that do not contain any metallic domains. Each point in the figure is the average over several (usually four) samples. That way, for example, absence of long-range metallic effects would be manifested by a value of unity, regardless of stripes' width. Likewise, if the only effect of the presence of gold or platinum is to enhance photodegradation, a monotonic decreasing curve, beginning with values greater than unity and decaying asymptotically to unity at very large widths, is expected. A fast glance over Figure 7 reveals a more complex behavior, characterized by a non-monotonic curve. For certain widths, not only that the presence of noble metals did not increase photoefficiency but, in fact, was detrimental. The effect of platinum seems to be different than that of gold. With narrow stripes (5 μm), both platinum and gold enhance photodegradation. Nevertheless, as the stripes' width increases, the degradation rate in samples containing platinum continues to increase, while that of samples containing gold decreases. Values go through extrema, where the relative efficiencies are 165% with Pt stripes (type VI) and 80% with Au stripes (type VI). Of interest are the values obtained with Pt stripes of 160 μm (60 ± 15%). Here, a second extremum is expected at further larger widths since the value for infinite width should be unity. A comparison between type V and type VI platinized samples does not reveal any significant effect of the substrate (silicon or titanium dioxide) onto which

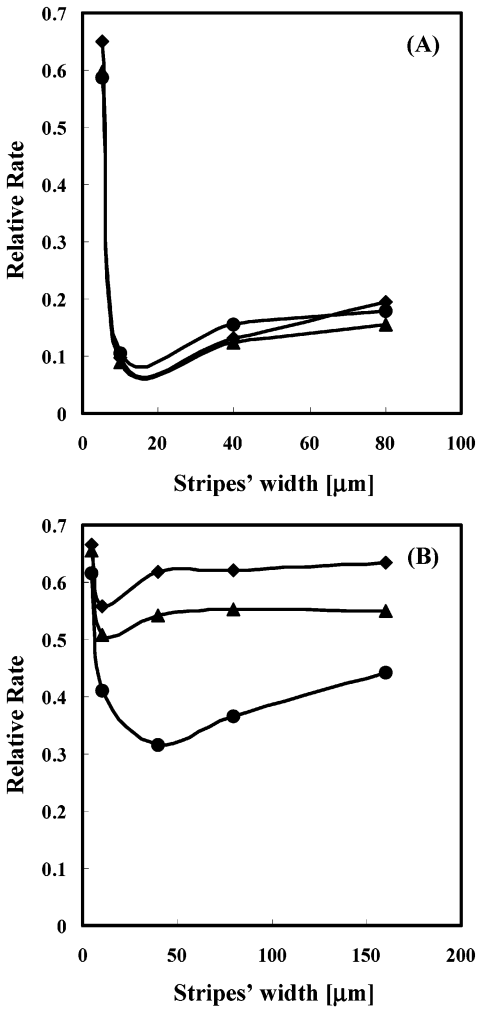

Figure 9. Degradation rates, relative to those of type-I samples, as a function of the stripes' width, at various degradation coordinates: (◆) initial rate, (▲) 20% consumption, (●) 50% consumption. (A) type-VI [Au], 1% RH; (B) type-VI [Pt], 1% RH.

the metal was deposited. In contrast, for gold-containing samples, the type VI samples gave consistently higher rates than the type V samples.

The long-range effects of the metallic stripes were tested also under low (1%) RH, where direct oxidation might be the dominant mechanism. The relative photodegradation rates, calculated at 20% of degradation, are presented in Figure 8. The most striking observation is the detrimental effect of the metallic stripes (noticed by relative rate values lower than 1), obtained at all of the measured distances, for both metals and sample types. Under low humidity, the relation between the photodegradation rates and the stripes' width is similar for both metals, with the relative efficiency being much lower for samples containing gold stripes. Relative efficiencies begin with 0.6 at 5 μm width, drop down, and increase. Here, again, a value of unity is expected at infinite width.

As mentioned above, the relation between the influence of the metallic stripes and the width of the stripes was presented based on rates calculated at 20% consumption. Because, in principle, such effects could be manifested differently at different stages of the photocatalytic degradation process, the curves portrayed in Figures 7 and 8 had to be constructed also at other reaction coordinates. Close examination of such sets of graphs revealed exactly the same behavior for all reaction coordinates, regardless of the type of metal, RH, or the type of the sample. This consistency is demonstrated in Figure 9A for type VI samples containing gold stripes under low humidity, where the normalized relative efficiency vs stripes' width is given for initial rates, rates at 20% consumption, and rates at 50% consumption. The only case where one could observe some difference between the curves was that of samples containing platinum stripes (both type V and type VI), under low humidity (Figure 9B), where the relative rate decreased with the propagation of the reaction. In other words, for Pt stripes under low humidity, the detrimental effect of the metal becomes more and more pronounced as the degradation proceeds.

4. Discussion

The effects of nano-domains of noble metals on the photoefficiency of titanium dioxide particles are well-documented in the literature and are the subject of intensive research.[33,34] In contrast, not much was known so far on long-range effects. As described in the previous section, such effects, which give rise to quite a complex behavior, do exist. In the following section, we will address these effects, trying to explain their richness and complexity.

The techniques described in this paper provide a unique way to control the location of the organic molecules, not only in terms of the substrate on which the contaminants reside but also in terms of exact distances and domain size. This is done by immobilizing the organic model systems (the SAMs) on well-defined domains; a way that is quite different from most measurements with metal-loaded nanoparticles, where the actual location of the organic molecules is generally unknown and where there is no practical means to control distances and loadings. Along this line, the metallic effects can be divided into two: effects on the degradation of organic molecules attached to metallic microdomains and effects on the photodegradation of molecules anchored to the photocatalyst itself.

SAMs on domains of noble metals, such as platinum or gold, located at the vicinity of titanium dioxide were found to be resistant toward photocatalysis regardless of the domains' size (Figure 5). In contrast, SAMs on domains of the native oxide of silicon, located at the vicinity of titanium dioxide, photodegraded rapidly (Figure 4), manifesting the ability of the oxidizing species to move from the titanium dioxide, where they were formed, into the inert domains.[29,35] The degradation of SAMs on aluminum (in fact on its native oxide) represents a third class where degradation occurs, however, at very low rate in comparison to that on silicon. These variations in the degradation rates correlate well with the reaction probabilities between gas phase $OH^{\bullet}$ radicals and these surfaces at room temperature.[36] Here, the reaction probability of hydroxyl radicals with titanium dioxide was 2×10^{-4}, 2×10^{-3} with silicon dioxide, 5×10^{-3} with alumina, and only 3×10^{-2} with gold. The observation that molecules attached to gold or platinum domains located at the vicinity of titanium dioxide do not degrade can be quite significant from a practical point of view. A practical example for the importance of this observation is the construction of selective photocatalysts, whose selectivity is based upon mass transfer enhancement. Here, monolayers of molecules that have selective affinity toward specific contaminants are constructed on inert domains in the vicinity of titanium dioxide. During operation, the contaminants first physisorb on these inert molecular recognition sites and then surface diffuse to the photocatalytic domains.[37] No wonder that care has to be taken to prevent the degradation of the molecular recognition sites, which are organic by nature.

The long-range effect of metals on the photodegradation of SAMs attached to titanium dioxide seems to be much more

complex. Although charge separation definitively has an important role (as demonstrated in the case of the buried layer, Figure 6), this, by itself, cannot explain why at certain distances the beneficial effect is changed into a detrimental one or the dependence of this effect on the humidity, as is demonstrated by the difference between Figure 7 and Figure 8.

Instead, it is proposed that the observed phenomena reflect a balance between the influence of several players, some of which are detrimental while others are beneficial. Moreover, the distance dependence of each player might be different and affected by external conditions. The rationalization of the above-mentioned results is based upon the well-established notion that the species responsible for the degradation, at least in its early stages, are hydroxyl radicals (eq 2), formed from holes and adsorbed water (eq 1). That this is the case also in the degradation of the SAMs is evident by comparing the rates under RH of 40% to those under RH of 1%, where the initial rate was half. Direct oxidation by holes cannot be ruled out under low humidity conditions.

$$h^+ + H_2O \rightarrow OH^\bullet + H^+ \quad (1)$$

$$OH^\bullet + R \rightarrow R^\bullet + H_2O \quad (2)$$

As was shown long ago,[38] oxygen is important for stripping the electrons and producing superoxide ions (eq 3) or hydroperoxy radicals (eq 4); otherwise, the recombination rate might be too high. However, the role of oxygen extends beyond electron stripping. It was established that *n*-alkanes undergo photodegradation by a mechanism that involves a reaction between oxygen and alkyl radicals, thus forming organoperoxy radicals (eq 5), which react further with the hydroperoxy radicals (eq 6) to yield organohydrotetraoxides that disintegrate, releasing CO_2 and water.[39] Another possibility is the abstraction of hydrogen from the organic molecule by a HO_2 radical. On the basis of the similarity between *n*-octane and the SAMs in question, it is sensible to assume a similar mechanism. Hence, we may conclude that in the photodegradation of SAMs made of long alkyl chains, not only holes (or trapped holes, as OH radicals are often perceived) play a role but also electrons.

$$e^- + O_2 \rightarrow OO^- \quad (3)$$

$$OO^- + H^+ \rightarrow {}^\bullet OOH \quad (4)$$

$$R^\bullet + O_2 \rightarrow R'OOR'' \quad (5)$$

$$R'OOR'' + {}^\bullet OOH \rightarrow R'CH(OOOOH)R'' \rightarrow R'''CHO + CO_2 + H_2O \quad (6)$$

Having this photodegradation mechanism in mind, one may now analyze the effect of noble metals on this scheme. As is well-accepted, electrons may be captured by the metal, thus improving charge separation, and eventually larger yield of OH radicals. Once on the metallic domains, electrons may reduce oxygen molecules, thus producing superoxide ions or hydroperoxy radicals, in the same manner described before but on the metal surface.[6] For hydroperoxy radicals to be formed on the metal, H^+ ions formerly formed on the titanium dioxide domains have to diffuse to the metal sites. Long-range diffusion of this species is possible, with a diffusion coefficient that tends to increase with humidity.[40] Once superoxide ions or hydroperoxy radicals are formed, they may diffuse to the titanium dioxide, where they may participate in reaction 6.

According to this explanation, noble metals may enhance photodegradation by promoting the production of OH radicals but on the other hand might reduce the photodegradation rate if, for some reason, electrons, in the form of hydroperoxy radicals or superoxide ions, do not return to the titanium dioxide domains. This may rationalize the detrimental effect found for very large distances.

It is conceivable that the diffusion coefficient of ${}^\bullet OOH$ on titanium dioxide is larger than that of OO^-, especially since the latter was claimed to have very low mobility on the surface.[41,42] If this difference is large enough, such that back-diffusion is dominated by that of ${}^\bullet OOH$, the diffusion of H^+ to the metal can become the bottleneck of the process. The fact that at dry environment the metallic effect is detrimental for all stripes' widths is then explained by the lower diffusion coefficient of hydrogen species measured on oxide surfaces under dry conditions.[40]

It was shown[43] that superoxides may produce hydroxyl radicals by a mechanism involving the reduction of H_2O_2, a species that might be formed from two superoxide anions and two H^+. Indeed, the addition of 0.2 mM H_2O_2 during a photocatalytic reaction tripled the concentration of $OH^\bullet$ radicals.[42] Nevertheless, if one takes into account the fact that in the absence of added hydrogen peroxide the concentration of H_2O_2 is limited by the concentration of superoxides, one has to conclude that the contribution of such a reductive mechanism to the production of $OH^\bullet$ radicals is negligible.

As demonstrated in Figures 7 and 8, the metallic effect of type V samples was found to be similar to that of type VI samples. While this similarity acts to support statistics, it is also suggesting that the titanium dioxide−metal interface has only a limited effect on buried contacts. Obviously, this conclusion should be drawn only for electrons or holes since when it comes to the metal−titanium dioxide interface at the air-exposed surface both types of samples are exactly the same. In fact, as mentioned in the discussion of the photodegradation of SAMs on metals, this interface may reduce $OH^\bullet$ concentration. Taken that the length of the interface scales such as one over the stripes' width, it is expected that such an effect would diminish with increasing the width.

The higher Schottky barrier at the Pt/TiO_2 interface as compared with the Au/TiO_2 interface explains why under all conditions the relative photodegradation rates in samples containing platinum were higher than those in the corresponding samples with gold. However, the differences between the two metals were not only in the values of the relative rates but also in the dependence on the width of the stripes. Here, for Pt-containing samples, the photoefficiency increased with the stripes' width (up to 40 μm) while for Au-containing samples, the photoefficiency decreased within similar range. This difference can be explained on the basis of the much higher efficiency of platinum in H_2 production in comparison with gold.[44] From the point of view of the degradation of the SAMs, the ability of platinum to evolve H_2 is destructive, since it consumes electrons that otherwise could have been utilized for degradation in the form of superoxide ions or hydroperoxy radicals. This is a detrimental effect, which accompanies the beneficial effect of charge separation. The H_2 production from H^+ occurs most likely at the interface between the metal and the titanium dioxide, because this is where electrons accumulate. Because the relative importance of the interfaces decreases in our experiments with the width of the domains, this detrimental effect in the platinized samples should decrease with the width. This decrease in the detrimental effect should give rise to an

enhancement in the overall efficiency when combined with the "charge separation effect", which is a beneficial effect that decays slower with increasing the width. This explanation is in line with the fact that under low humidity, where the amount of H_2 production is negligible, the efficiency decreases as a function of width for samples containing platinum as well as for samples containing gold (Figure 8).

As was demonstrated in Figure 9, the metallic effect was independent of the reaction coordinate. This suggests a quasi steady state with respect to each of the components that affect the degradation rate. The only exceptions are samples containing platinum stripes under dry conditions (types V and VI), where the metal showed a detrimental effect, which became more pronounced with reaction coordinate. It is believed that this case represents an effective enhancement in recombination, which occurs due to accumulation of charge that cannot be spilt away in the form of OOH, due to the low surface moisture.

Conclusion

In this paper, evidence for long-range effects of noble metals on the photodegradation of SAMs anchored to titanium dioxide was presented. These effects were explained by a mechanism that includes not only the transfer of electrons but also the front and back transfer of ions and radicals. While charge separation is the common denominator of almost all papers discussing metallic effects in powders, the presented work suggests that the diffusion of H^+ from the photocatalyst to the metal and the back-diffusion of reduced oxygen species such as hydroperoxy radicals may also play an important role. It is further suggested that although charge separation is beneficial in promoting the production of hydroxyl radicals needed for the first steps of photocatalysis, charge separation might also become detrimental, under conditions that decrease the back-diffusion of reduced species needed at later stages.

Acknowledgment. This work was funded by the Israeli Ministry of Science, by the Israel Science Foundation, and by the 5th Program of the European Commission (INCOMED). We are indebted to Dr. R. Brenner and to Mr. G. Shemer for their help.

References and Notes

(1) See, for example, (a) Holmann, M. M. *Photodegradation of Water Pollutants*; CRC Press: Boca Raton, FL, 1996. (b) Blake, D. M. *Bibliography of Work on the Photocatalytic Removal of Hazardous Compounds from Water and Air*; NREL: Golden, CO, 1999. (c) Mills, A.; Le Hunte, S. *J. Photochem. Photobiol. A* **1997**, *108*, 1. (d) Fujishima, A.; Hashimoto, K.; Watanabe, T. *TiO_2 Photocatalysis*; BKC: Tokyo, 1999. (e) Ollis, D. F. *Catal. Technol*. **1998**, *2*, 149. (f) Litter, M. I. *Appl. Catal. B* **1999**, *23*, 89.

(2) Henrich, V. A.; Dresselhaus, D.; Zeiger, H. *J. Phys. Rev. Lett.* **1976**, *36*, 1335.

(3) Cermenati, L.; Pichat, P.; Chantal, G.; Albini, A. *J. Phys. Chem. B* **1997**, *101*, 2650.

(4) Hoffmann, M. R.; Martin, S. T.; Choi, W.; Bahnemann, D. W. *Chem. Rev.* **1995**, *95*, 69.

(5) Bahnemann, D. W.; Hilgendorff, M.; Memming, R. *J. Phys. Chem. B* **1997**, *101*, 4265.

(6) Gerischer, H.; Heller, A. *J. Phys. Chem.* **1991**, *95*, 5261.

(7) Goldstein, S.; Czapski, G.; Rabani, J. *J. Phys. Chem.* **1994**, *98*, 6586.

(8) Wang, C. Y.; Liu, C. Y.; Zheng, X.; Chen, J.; Shen, T. *Colloid Surf. A* **1998**, *131*, 271.

(9) Li, X. Z.; Li, F. B. *Environ. Sci. Technol.* **2001**, *35*, 2381.

(10) Sclafani, A.; Palaminisana, L.; Marcí, G.; Venezia, A. *Sol. Energy Mater. Sol. Cells* **1998**, *51*, 203.

(11) Yang, J. C.; Kim, Y. C.; Shul, Y. G.; Shin, C. H.; Lee, T. K. *Appl. Surf. Sci.* **1997**, *121/122*, 525.

(12) Sclafani, A.; Herrmann, J.-M. *J. Photochem. Photobiol. A: Chem.* **1998**, *113*, 181.

(13) Wang, C.-M.; Heller, A.; Gerischer, H. *J. Am. Chem. Soc.* **1992**, *114*, 5230.

(14) Anpo, M. *Catal. Surv. Jpn.* **1997**, *1*, 169.

(15) Linsebigler, A. L.; Lu, G.; Yates, J. T. *Chem. Rev.* **1995**, *95*, 735.

(16) Sakata, T.; Kawai, T.; Hashimoto, K. *Chem. Phys. Lett.* **1982**, *88*, 50.

(17) Ozen, I.; Uner, D. *Stud. Surf. Sci. Catal.* **2001**, *133*, 445.

(18) Falconer, J. L.; Magrini-Bair, K. A. *J. Catal.* **1998**, *179*, 171.

(19) Bamwenda, G. R.; Tsubota, S.; Kobayashi, T.; Haruta, M. *J. Photochem. Photobiol. A: Chem.* **1994**, *77*, 59.

(20) Ohtani, B.; Iwai, K.; Nishimoto, S.-I.; Sato, S. *J. Phys. Chem. B* **1997**, *101*, 3349.

(21) Courbon, H.; Hermann, J. M.; Pichat, P. *J. Phys. Chem.* **1984**, *88*, 5210.

(22) Subramanian, V.; Wolf, E.; Kamat, P. *J. Phys. Chem. B* **2001**, *105*, 11439.

(23) Kennedy, J. C., III; Datye, A. K. *J. Catal.* **1998**, *179*, 375.

(24) Bamwenda, G. R.; Tsubota, S.; Nakamura, T.; Haruta, M. *J. Photochem. Photobiol. A: Chem.* **1995**, *89*, 177.

(25) Linsebigler, A.; Rusu, C.; Yates, J. R. *J. Am. Chem. Soc.* **1996**, *118*, 5284.

(26) Paz, Y.; Luo, Z.; Rabenberg, L.; Heller, A. *J. Mater. Res*. **1995**, *10*, 2842.

(27) Paz, Y.; Heller, A. *J. Mater. Res.* **1997**, *12*, 2759.

(28) Sagiv, J. *J. Am. Chem. Soc*. **1980**, *102*, 92.

(29) Haick, H.; Paz, Y. *J. Phys. Chem. B* **2001**, *105*, 3045.

(30) Zemel, E.; Haick, H.; Paz, Y. *J. Adv. Oxid. Technol.* **2002**, *5* (1), 27.

(31) Ulman, A. *An Introduction to Ultrathin Organic Films*; Academic Press: London, 1991.

(32) Hiraki, A. *Surf. Sci. Rep.* **1984**, *3*, 357.

(33) Dawson, A.; Kamat, P. V. *J. Phys. Chem. B* **2001**, *105*, 960.

(34) Highfield, J. G.; Pichat, P. *New J. Chem.* **1989**, *13*, 61.

(35) Choi, W.; Lee, M. C.; Cho, S. The 14th International Conference on Photochemical Conversion and Storage of Solar Energy, Sapporo, Japan, 2002; p W2-P-27.

(36) Suh, M.; Bagus, P. S.; Pak, S.; Rosynek, M. P.; Lunsford, J. H. *J. Phys. Chem. B* **2000**, *104*, 2736.

(37) Ghosh-Mukerji, S.; Haick, H.; Schvartzman, M.; Paz, Y. *J. Am. Chem. Soc.* **2001**, *123*, 10776.

(38) Anpo, M.; Aikawa, N.; Kubokawa, Y.; Che, M.; Louis, C.; Gianello, E. *J. Phys. Chem.* **1985**, *89*, 5689.

(39) Schwitzgebel, J.; Ekerdt, J. G.; Gerischer, H.; Heller, A. *J. Phys. Chem.* **1995**, *99*, 5633.

(40) Roessner, F.; Roland, U. *J. Mol. Catal.* **1996**, *112A*, 401.

(41) Ishibashi, K.-I.; Nosaka, Y.; Hashimoto, K.; Fujishima, A. *J. Phys. Chem.* **1998**, *102*, 2117.

(42) Hirakawa, T.; Nosaka, Y. *Langmuir* **2002**, *18*, 3247.

(43) Shibata, H.; Ogura, Y.; Sawa, Y.; Kono, Y. *Biosci. Biotechnol. Biochem*. **1998**, *62*, 2306.

(44) Haripriya, S.; Sangaranarayanan, M. V. *Langmuir* **2002**, *18*, 5572.